JOURNAL OF SPACECRAFT AND ROCKETS
Vol. 38, No. 6, November–December 2001

Using Motorized Tethers for Payload Orbital Transfer

Spencer W. Ziegler* and Matthew P. Cartmell†
University of Glasgow, Glasgow, Scotland G12 8QQ, United Kingdom

The concept of symmetrical double-ended motorized spinning tethers for use as orbital transfer vehicles is introduced. The orbital elements of a payload released from above and below a hanging, prograde librating, and prograde spinning tether are derived and employed to evaluate the effectiveness of the three tether types along with their optimum configurations for payload transfer. A new ratio, the efficiency index, is defined as the altitude gain or loss half an orbit after tether release per tether length. The motorized tether is found to perform best and also most efficiently, improving by two orders of magnitude on the librating tether, which, in turn, improves on the hanging tether by a factor of two. A long motorized tether on a circular orbit can transfer an upper payload from a low to a geostationary Earth orbit by employing relatively high motor torque and a safety factor on the tether strength close to unity.

Nomenclature

A	=	cross-sectional area of tether, m^2
L	=	tether length from center of mass (COM) to payload, m
l	=	tether length from COM to a point along the tether, m
M_M, M_P	=	motor and payload mass, kg
P	=	power source, W
r_{AP}, r_{PE}	=	apogee and perigee radius of payload's orbit after release, m
r_C	=	circular orbit radius of COM at payload release, m
r_M, r_P	=	radius of motor and payload, m
r_{Ti}, r_{To}	=	inner and outer radius of tether tube, m
r_0, r_π	=	orbital radius of payload at release and half an orbit after release, m
S.F.	=	safety factor, dimensionless
T, U	=	kinetic and potential energy, J
U_M	=	potential energy of motor, J
U_{P1}, U_{P2}	=	potential energy of upper and lower payload, J
U_{T1}, U_{T2}	=	potential energy of upper and lower tether, J
v_0	=	tangential velocity of payload at release, m/s
Δr_π, $\Delta r_\pi / L$	=	performance, m, and efficiency index, dimensionless
ΔV	=	velocity increment, m/s
ε	=	orbit eccentricity, dimensionless
$\dot{\theta}$, $\dot{\psi}$	=	angular orbital and pitch velocity, rad/s
θ_{MAX}	=	maximum libration angle between tether and gravity vector, rad
μ	=	product of gravitational constant and Earth's mass, m^3/s^2
ρ, σ	=	density, kg/m^3, and ultimate tensile strength of tether, N/m^2
τ	=	motor torque, Nm
ψ	=	pitch angle, rad
$\dot{\psi}_v$	=	angular pitch velocity when tether is aligned along gravity vector, rad/s

Received 10 August 2000; presented as Paper 2000-4529 at the AIAA/AAS Astrodynamics Specialist Conference, Denver, CO, 14–17 August 2000; revision received 21 May 2001; accepted for publication 25 May 2001.

*Graduate Student, Department of Mechanical Engineering. Student Member AIAA.
†Professor, Department of Mechanical Engineering. Member AIAA.

Introduction

TETHERED masses, orbiting a source of gravity in space, possess the same orbital angular velocity as the overall center of mass (COM). As the upper payload is released from a hanging tether, i.e., always aligned along the gravity vector, the upper payload carries more angular velocity than it requires to stay on that circular orbit, but because the upper payload does not have enough energy to escape the Earth's gravity, the upper payload goes into an elliptical orbit with the release point being the perigee of the orbit, as shown in Fig. 1. Similarly, the lower payload does not have enough velocity to stay on its circular orbit when it is released, and so it too goes into an elliptical orbit but this time with the release point being the apogee of the orbit. Half an orbit later the upper payload reaches its apogee and is hence further from Earth than it was at the point of release. Upon reaching the perigee of the orbit, the lower payload is closer to the Earth than it was at release. Thus, the upper and lower masses released from a hanging tether are respectively raised and lowered. A prograde swing or spin will add velocity to the upper payload and decrease the velocity of the lower. A retrograde swing or spin will decrease the upper payload's velocity, which means the payload at release will either have more, just the correct amount of or not enough velocity to stay on its original orbit. The release point, therefore, will either be the perigee or the apogee of the elliptical orbit or it could stay on the original circular orbit. The reverse holds for the lower payload experiencing a retrograde spin or swing, which will have either not enough, just the right amount of, or too much velocity to stay on orbit. The release point will, consequently, be the apogee or perigee of an elliptical orbit, or it could stay on its circular orbit. For maximum apogee altitude gain and perigee altitude loss the most desirable tether motion has to be either a prograde swing, or spin as more tangential velocity is added to the upper and subtracted from the lower payload. The optimum release point for a swinging or spinning tether is when the tether is aligned along its gravity vector and when the motion itself is coplanar with the orbital plane. The radial separation, Δr_π, between the payload half an orbit after release and the tether COM's circular orbital radius at release is greater than the tether's length L for orbit raising and less than L for orbit lowering.

Colombo et al.[1] was one of the first to propose raising or lowering a payload's orbit with momentum exchanging tethers. A hanging tether in a circular orbit was considered by Bekey and Penzo[2] for transferring a payload from low Earth orbit (LEO) to geostationary Earth orbit (GEO). However, a potentially dangerous drop in the shuttle's perigee after release and resulting tether tension exceeding any known material were cited as problems against this proposal. Kelly[3] suggested tethering the space shuttle to its external fuel tank at separation in order to raise the shuttle's orbit and to simultaneously deorbit the tank, concluding that the proposal was attractive but control stability and guidance dispersion issues of the external tank had to be addressed. Lorenzini et al.[4] investigated propelling a payload from LEO to GEO using a two-stage tether system, where the transfer time was found to be comparable to that of a chemical

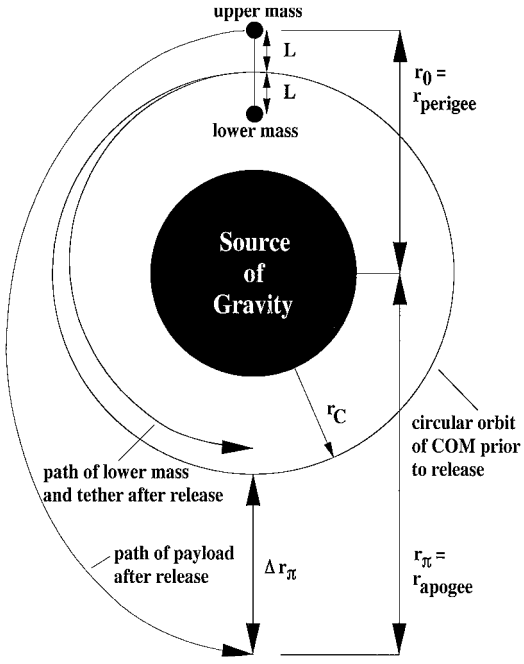

Fig. 1 Orbital elements of a payload released above a symmetrical tether.

upper stage. Their study claims that a two-stage tether system is more competitive on a mass basis than a chemical-propellantupper stage after two orbital transfers.

The commonly quoted results in the literature for Δr_π, treating the case of upper payload release, are[2,4–7]

$$\Delta r_\pi \approx 7L, \qquad \text{hanging tether} \tag{1}$$

$$\Delta r_\pi < 14L, \qquad \text{swinging tether} \tag{2}$$

$$\Delta r_\pi > 14L, \qquad \text{spinning tether} \tag{3}$$

Bekey[8] claimed the spinning tether release generates $\Delta r_\pi > 25L$. Cosmo and Lorenzini[7] give a formula to calculate Δr_π for a swinging release, provided the tether and its end mass remain on the original circular orbit:

$$\Delta r_\pi \approx \left(7 + \sqrt{48}\sin\theta_{\text{MAX}}\right)L \tag{4}$$

where θ_{MAX} is positive for prograde and negative for retrograde rotation. Cosmo and Lorenzini[7] state that Eqs. (1–4) only hold as long as $\Delta r_\pi \ll r_C$.

Kyroudis and Conway[9] tried to improve the orbital transfer achieved with tethers by examining the use of a librating tethered dumbbell system on an elliptical orbit for satellite transfer to GEO. Reference 9 reported that the ΔV savings and payload gain compared to a Hohmann transfer improve with higher eccentricity orbits, longer tether lengths, and faster deployment speeds for similar initial periapse altitudes. Kumar et al.[10] studied the effects of various tether deployment schemes as well as the out-of-plane libration on payload orbit raising of a tethered dumbbell on an elliptical orbit. For the swinging in-plane dumbbell on a circular orbit, they derived the following expression:

$$\Delta r_\pi \approx (7 + 4\dot{\psi}_v/\dot{\theta})L \tag{5}$$

which holds for both swinging and spinning systems assuming $L \ll r_C$. Contrary to the analysis of Kyroudis and Conway,[9] who had observed an increase in apogee altitude of the payload with deployment rate, Kumar et al.[10] found from their three-dimensional analysis that the apogee altitude gain vs deployment rate relationship is characterised by nontrivial peaks and valleys. Furthermore, Kumar et al.[10] claimed that nonzero initial roll angles have little effect on the orientation of the payload orbit after its release.

Equations (4) and (5) support the literature result that a payload released above a hanging tether rises approximately seven times the tether's length half an orbit later. This result is independent of the COM's orbital radius, despite the tangential orbital velocity being a function of the orbital radius. Equation (4), moreover, is independent of both the facility's orbital radius and payload mass, where both should affect the payload's momentum. Equation (5) takes the angular orbital and pitch velocities into account but is not directly dependent on the orbital radius. Motivated by these discrepancies, this paper significantly reassesses the results given in Eqs. (1–5), derives new expressions for the Δr_π of payloads released from hanging, prograde librating and prograde spinning tethers, introduces symmetrical double-ended motorized tethers for use as orbital transfer vehicles, describes their most effective configurations, and evaluates their effectiveness at payload orbital transfer.

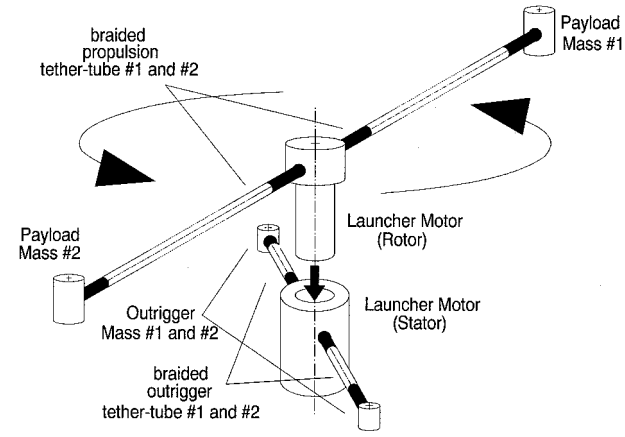

Fig. 2 Schematic of symmetrical double-ended motorized tether concept, as suggested by Cartmell and Ziegler.[12]

Concept of Symmetrical Double-Ended Motorized Tethers

Exploiting momentum exchange tethers to propel payloads is essentially a passive procedure as the amount of ΔV achievable is dependent on the initial conditions, eccentricity of the orbit, the properties and geometry of both the tether and payload. Cartmell[11] proposed the inclusion of a motor to intentionally spin the tethered system, thereby, giving the opportunity of generating an additional ΔV. Two "propulsion" tethers are attached in a symmetrical fashion, as suggested by Cartmell and Ziegler[12] and shown in Fig. 2, to the casing of an electric motor, which is located at the COM and obtains its electricity from solar panels or a fuel cell. A payload is attached to each remaining free end of the tether. Once the tether is fully deployed, the motor is energized applying, thereby, a torque to the tethers. Because of their flexibility and lack of inherent static stiffness, the tethers cannot transmit the torque to the payloads at first. Two small tangential boosters in each payload are needed to provide thrust during the initial stages of the tether spin-up to account for the lack of centripetal acceleration required to keep the tethers taught and hence stop the tethers winding themselves around the motor. As the tethered system's acceleration caused by the motor builds up about the COM, the boosters can gradually be switched off. Eventually the tangential velocity of the payloads reaches the required level and the payloads are released onto a desired tangential path. If the payloads and tethers are identical and symmetrically attached, then upon simultaneous payload release the tethered facility's COM will not shift. However, with the facility's new mass moment of inertia and perturbational detachment forces some additional boost will be required to maintain the facility's altitude. The motor consists of a rotor, which is attached to the propulsion tethers and contains the drive motor, power supplies, and control systems, and a stator, connected to the rotor by means of a suitable bearing. The stator provides the necessary backrotation that is required for the rotor to spinup in a friction-free environment. The stator's angular acceleration is controlled by deploying a pair of shorter "outrigger" tethers, which terminate in end masses, from the stator housing, thus increasing the stator's mass moment of inertia.

Orbital Elements of the Payload After Release

This paper considers the release of both the upper and lower payloads from a hanging, prograde librating, and prograde spinning

symmetrical tether. As the tethered facility's COM does not shift upon payload release, the results are applicable to those given in the literature, which makes the assumption that the COM's change in altitude after release is negligible.[7] It is assumed that the motorized tether facility is on a circular orbit about the Earth, the Earth's gravitational field is spherical, environmental perturbations are negligible, the tether's motion is coplanar with the orbital plane, the tethers are rigid, the cross-sectional area of the tether is constant, the tethers are fully deployed before payload release is considered, and the payloads are released when the tether is aligned along its gravity vector. This final assumption implies that the release point is either the perigee or apogee of the payload's elliptical orbit.

Considering the velocity of the released payload at perigee or apogee, as given by Chobotov,[13] substituting in the appropriate semilatus rectum, squaring both sides, rearranging in terms of ε, and substituting into the relation $r_{\mathrm{AP}}(1-\varepsilon) = r_{\mathrm{PE}}(1+\varepsilon)$ leads to

$$\Delta r_\pi = r_\pi - r_C = \frac{r_0^2 v_0^2}{2\mu - r_0 v_0^2} - r_C \tag{6}$$

Equation (6) represents the distance, half an orbit after the tether has released the payload, between the payload and the facility's orbit at the time of release for any form of release obeying the preceding assumptions. Inserting the payload's orbital radius and tangential velocity at the point of release from a hanging tether into Eq. (6) for the upper payload gives

$$\Delta r_\pi = \frac{(r_C + L)^4}{2r_C^3 - (r_C + L)^3} - r_C \tag{7}$$

and similarly for the lower payload

$$\Delta r_\pi = \frac{(r_C - L)^4}{2r_C^3 - (r_C - L)^3} - r_C \tag{8}$$

Inserting the payload's orbital radius and tangential velocity when released from a prograde swinging or spinning tether into Eq. (6) for the upper payload gives

$$\Delta r_\pi = \frac{(r_C + L)^2[(r_C + L)\dot\theta + L\dot\psi]^2}{2\mu - (r_C + L)[(r_C + L)\dot\theta + L\dot\psi]^2} - r_c \tag{9}$$

and similarly for the lower payload

$$\Delta r_\pi = \frac{(r_C - L)^2[(r_C - L)\dot\theta - L\dot\psi]^2}{2\mu - (r_C - L)[(r_C - L)\dot\theta - L\dot\psi]^2} - r_c \tag{10}$$

Assuming $L \ll r_C$ implies $\delta \ll 1$, where $\delta = L/r_C$ and allows binomial expansion to be applied to Eqs. (7–10), giving to $\mathcal{O}(\delta)$

$$\Delta r_\pi \approx 7L \tag{11}$$

$$\Delta r_\pi \approx -7L \tag{12}$$

$$\Delta r_\pi \approx (7 + 4\dot\psi/\dot\theta)L \tag{13}$$

$$\Delta r_\pi \approx -(7 + 4\dot\psi/\dot\theta)L \tag{14}$$

and to $\mathcal{O}(\delta^2)$

$$\Delta r_\pi \approx (7 + 30L/r_C)L \tag{15}$$

$$\Delta r_\pi \approx (-7 + 30L/r_C)L \tag{16}$$

$$\Delta r_\pi \approx \left[7 + 30L/r_C + 4\dot\psi/\dot\theta + 2Lr_C^2\dot\psi(18\dot\theta + 5\dot\psi)/\mu\right]L \tag{17}$$

$$\Delta r_\pi \approx \left[-7 + 30L/r_C - 4\dot\psi/\dot\theta + 2Lr_C^2\dot\psi(18\dot\theta + 5\dot\psi)/\mu\right]L \tag{18}$$

As can be seen, the literature expressions, Eqs. (1) and (5), are obtained from Eq. (6). In contrast to Eq. (1), which is linear and solely dependent on L, Eq. (7) is a nonlinear expression and a function of r_C and L. Equation (9), moreover, is dependent on r_C, L, μ, $\dot\psi$, and $\dot\theta$, whereas Eq. (5) is solely dependent on L, $\dot\psi$, and $\dot\theta$. The second-order simplification in Eqs. (15) and (16) gives a mission designer a better insight into the most effective orbital position for the hanging tether than the first-order terms in Eqs. (11) and (12). To obtain $\dot\psi$ for the preceding expression, it is necessary to distinguish between cases where the motor is on or off.

Equation of Motion of Motorized Tether Facility

An untorqued tethered system on a circular orbit will hang, librate, or spin depending on the tether's initial conditions. However, this paper only treats the hanging and librating cases as the untorqued tether is presumed to have no initial angular velocity. $\dot\psi$ has to be obtained when the tether is precisely aligned along its gravity vector, i.e., when the tether is vertical, so that Eqs. (9), (10), (13), (14), (17), and (18) can be evaluated. An analytical expression for $\dot\psi$ is desirable, and so the equation of motion of the motorized tether is derived. As this paper focuses on the payload orbital transfer capabilities of motorized tethers, the stator and the outrigger tethers are neglected in the derivation, and the assumption is made that these are providing the necessary resistive torque to allow spin-up. The kinetic energy of the tether comprises both translation and rotation of each massive component in a relative rotating coordinate system about the Earth, giving

$$T = \frac{1}{12}\begin{pmatrix} 3\left[2M_M r_C^2 + 4M_P\left(L^2 + r_C^2\right) + \rho AL\left(L^2 + 4r_C^2\right)\right]\dot\theta^2 + 6L^2(4M_P + \rho AL)\dot\theta\dot\psi \\ + \left\{3M_M r_M^2 + 6M_P\left(2L^2 + r_P^2\right) + \rho AL\left[4L^2 + 3\left(r_{\mathrm{To}}^2 + r_{\mathrm{Ti}}^2\right)\right]\right\}\dot\psi^2 \end{pmatrix} \tag{19}$$

where the tether is treated as a tube, attempting to model the Hoytether concept.[14] The total potential energy U is the sum of the following:

$$U_{P1} = -\frac{\mu M_P}{\sqrt{r_C^2 + L^2 + 2r_C L\cos\psi}} \tag{20}$$

$$U_{P2} = -\frac{\mu M_P}{\sqrt{r_C^2 + L^2 - 2r_C L\cos\psi}} \tag{21}$$

$$U_M = -\frac{\mu M_M}{r_C} \tag{22}$$

$$U_{T1} = -\mu\rho A\int_0^L \left(r_C^2 + l^2 + 2r_C l\cos\psi\right)^{-\frac{1}{2}}\,\mathrm{d}l = \mu\rho A\,\ell n\frac{r_C(1+\cos\psi)}{L + r_C\cos\psi + \sqrt{r_C^2 + L^2 + 2r_C L\cos\psi}} \tag{23}$$

$$U_{T2} = -\mu\rho A\int_0^L \left(r_C^2 + l^2 - 2r_C l\cos\psi\right)^{-\frac{1}{2}}\,\mathrm{d}l = \mu\rho A\,\ell n\frac{r_C(1-\cos\psi)}{L - r_C\cos\psi + \sqrt{r_C^2 + L^2 - 2r_C L\cos\psi}} \tag{24}$$

Note that Eqs. (23) and (24) only hold when $\psi \neq \pi$. Substituting Eqs. (19–24) into Lagrange's equation gives

$$\left\{\frac{M_M r_M^2}{2}+M_P\left(2L^2+r_P^2\right)+\frac{\rho AL\left[4L^2+3\left(r_{\mathrm{To}}^2+r_{\mathrm{Ti}}^2\right)\right]}{6}\right\}\ddot{\psi}+\frac{\mu M_P r_C L\sin\psi}{\left(r_C^2+L^2-2r_C L\cos\psi\right)^{\frac{3}{2}}}-\frac{\mu M_P r_C L\sin\psi}{\left(r_C^2+L^2+2r_C L\cos\psi\right)^{\frac{3}{2}}}$$

$$-\mu\rho A\tan\frac{\psi}{2}\frac{r_C^2+L^2-r_C L(1-\cos\psi)+(L-r_C)\sqrt{r_C^2+L^2+2r_C L\cos\psi}}{r_C^2+L^2+2r_C L\cos\psi+(L+r_C\cos\psi)\sqrt{r_C^2+L^2+2r_C L\cos\psi}}$$

$$+\mu\rho A\cot\frac{\psi}{2}\frac{r_C^2+L^2-r_C L(1+\cos\psi)+(L-r_C)\sqrt{r_C^2+L^2-2r_C L\cos\psi}}{r_C^2+L^2-2r_C L\cos\psi+(L-r_C\cos\psi)\sqrt{r_C^2+L^2-2r_C L\cos\psi}}=\tau \tag{25}$$

Integrating Eq. (25) with respect to ψ, assuming the tether starts from rest, gives

$$\dot{\psi}=\pm\sqrt{\frac{2[(\psi_1-\psi_0)\tau-U[\psi_1]+U[\psi_0]]}{M_M r_M^2/2+M_P\left(2L^2+r_P^2\right)+\rho AL\left[4L^2+3\left(r_{\mathrm{To}}^2+r_{\mathrm{Ti}}^2\right)\right]/6}} \tag{26}$$

where the subscripts 0 and 1 represent the beginning and end states, respectively, and the square brackets the evaluation of U at each of these states. Equation (26) allows Δr_π to be determined analytically, and numerically integrating Eq. (25) provides a numerical answer for comparison. Libration results are obtained from Eqs. (25) and (26) by setting $\tau=0$.

Tether Strength and Spin-Up Criterion

When the tether is torqued, $\dot{\psi}$ can be obtained analytically from Eq. (26) or by numerically integrating Eq. (25). This approach gives the conditions under which the tether can be spun, the nature of the spin-up, and the time required to reach a desired velocity, but it does not give the maximum achievable velocity. For this an expression is needed that incorporates the tether's strength. A tether, holding a payload at one end and rotating about the other, will experience centripetal acceleration and a resulting tensile force. Equating the two, while assuming the gravity gradient effects are negligible, gives

$$M_P L\dot{\psi}^2+\rho A\dot{\psi}^2\int_0^L l\,\mathrm{d}l=F_{\mathrm{tension}}=\sigma A \tag{27}$$

yielding

$$\dot{\psi}=\sqrt{\frac{\sigma A}{L(M_P+\rho AL/2)}} \tag{28}$$

Equation (28) can be used to determine the orbital elements of a payload after release from a motorized tether facility, which unjustifiably assumes that the velocity obtained from Eq. (28) can be achieved when the tether aligns itself along the gravity vector. However, as the relatively slow dynamics occur over a large period of time the difference between the prediction of Eq. (28) and $\dot{\psi}$ at the last vertical position before reaching the value from Eq. (28), which will be within one full rotation, is very small. Nonetheless, the results obtained using Eq. (28) will represent the maximum achievable orbital elements for the given configuration. Using Eq. (28), furthermore, presumes that an initial condition exists where the tether is able to spin up. The Earth's gravity exerts a force on the tether and payload masses, which acts through the tether length, depending on the tether's orientation and direction of motion, as either an additive or resistive torque on the motor. If the motor's torque is not large enough to override the resulting gravity torque, the tether will simply librate rather than spin up. A symmetrical double-ended motorized tether with an initial starting angle between $-\pi/2\le\psi_0<\pi/2$ will spin up in a prograde manner as long as $\dot{\psi}$ from Eq. (26) is positive and real at $\psi_1=\pi/2$. Thus, the analytical spin-up criterion is given by

$$(\pi/2-\psi_0)\tau-U[\pi/2]+U[\psi_0]>0 \tag{29}$$

where as a result of symmetry only $-\pi/2\le\psi_0<\pi/2$ needs to be considered.

Definition of Performance and Efficiency Indices

Δr_π gives the distance, half an orbit after the tether releases the payload, between the payload and the facility's orbit at the time of release. Essentially Δr_π describes how well the tether facility performs at transferring the payload. In the case of apogee altitude gain, the larger Δr_π is, the better the tether's performance in payload raising, and in the case of perigee altitude loss, the smaller Δr_π is, the better the tether's performance in payload lowering. Hence, Δr_π can be defined as the tether's performance index. It is also of interest to know how well the tether is performing in relation to its own length. A new ratio $\Delta r_\pi/L$ is introduced here and defines the tether's efficiency index. In the case of apogee altitude gain, a more efficient tether will have a larger $\Delta r_\pi/L$, whereas in the case of perigee altitude loss $\Delta r_\pi/L$ will be smaller. With this distinction made a further aim of this paper is to investigate the validity of the literature's prediction of the efficiency index for given configurations.

Results and Discussion

Unless stated otherwise all of the results were generated with the following system parameters: $\mu=3.9877848\times10^{14}$ m^{3}s^{-2}, $M_P=1000$ kg, $M_M=5000$ kg, $r_M=r_P=0.5$ m, $L=50$ km, $r_C=6870$ km, $r_{\mathrm{Ti}}=4$ mm, $r_{\mathrm{To}}=6$ mm, $A=62.83$ mm^2, $\rho=970$ kg m^{-3}, $\sigma=3.25$ GPa, S.F. $=2$, $\psi_0=-0.9$ rad, $\psi_1=0$. The data for the tether are based on Spectra 2000. Numerical results were obtained by integrating Eq. (25) with $\tau=0$ in MATHEMATICA® with a fourth/fifth-order Fehlberg Runge–Kutta method and in MATLAB® with a fourth/fifth-order Runge–Kutta method using a relative error of 10^{-8} and 10^{-10}, respectively. Because of the long integration times required, the relative error needed to be smaller than 10^{-7} to avoid spurious results. Very good agreement was found between the results from both integrators, and results were found not to significantly differ when relative errors smaller than 10^{-8} were used.

Hanging Tether

The hanging tether results for the upper, Fig. 3, and lower, Fig. 4, payload release show the analytical, first- and second-order approximations of the performance and efficiency indices, Eqs. (7), (11), (15) and Eqs. (8), (12), (16), respectively. The efficiency and performance of the upper payload released from a hanging tether increases with larger L. As r_C increases, the indices are found to decrease, tailing off for larger r_C, which suggests the most efficient and best performing hanging tether for payload raising is one that is as close as possible to Earth with the longest possible length. Such a configuration would have to be optimized as this position in orbit experiences the greatest atmospheric drag. However, a change in L has a greater effect on performance and efficiency than altering the orbital radius, and thus it is L that dominates the design of the hanging tether. The constant efficiency index of seven predicted by Eq. (11) is, as Figs. 3c and 3d show, a lower bound.

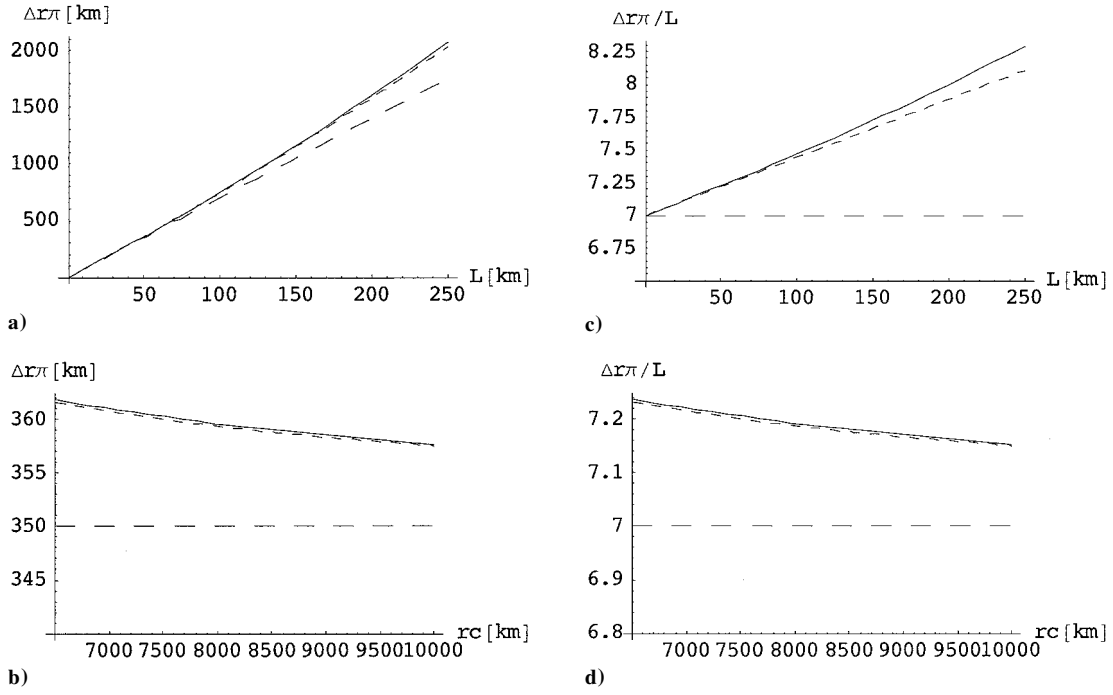

Fig. 3 Performance and efficiency of upper payload released from a hanging tether: ——, analytical, Eq. (7); - - -, first-order approximation, Eq. (11); and - - - -, second-order approximation, Eq. (15).

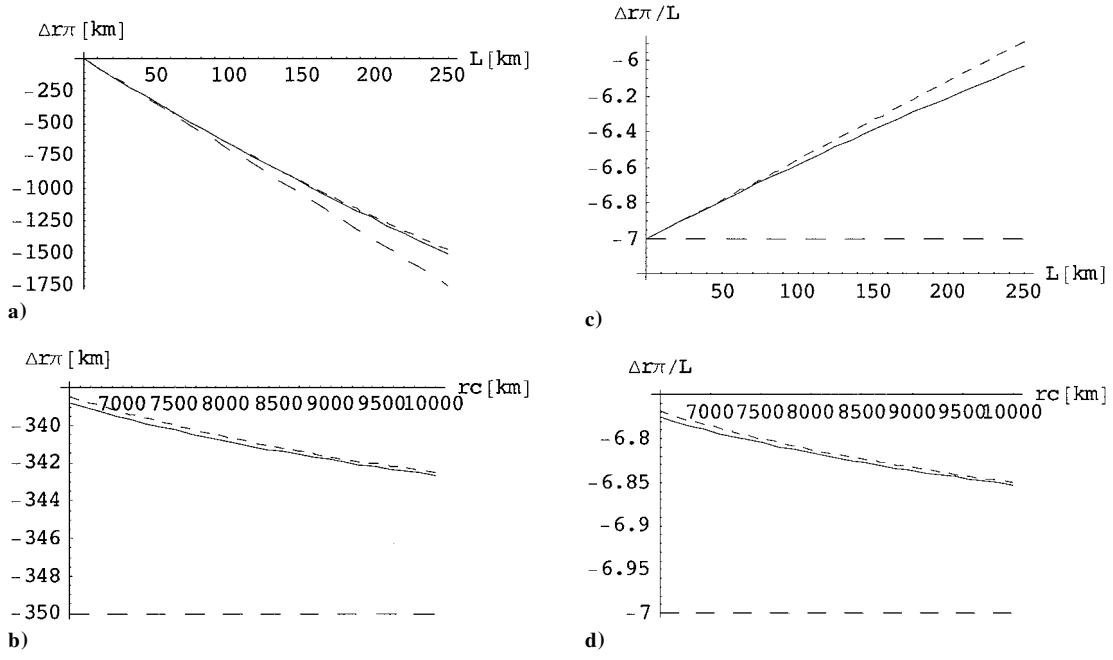

Fig. 4 Performance and efficiency of lower payload released from a hanging tether: ——, analytical, Eq. (8); - - -, first-order approximation, Eq. (12); and - - - -, second-order approximation, Eq. (16).

The results in Fig. 4 show that the requirements for high efficiency and performance in payload deorbiting from a hanging tether are different to those of payload raising. The performance of a lower payload release improves with larger L and r_C, whereas the efficiency drops with larger L and increases with greater r_C. A high-performance hanging tether for payload deorbit would, therefore, be as far as possible from Earth with a large tether length. Similarly, for efficient payload deorbit the tether is as far as possible from Earth but with a tether length that is as short as possible. As before, altering L has a greater effect on performance and efficiency than changing the orbital radius. The constant efficiency index of negative seven predicted by Eq. (12) is, as Figs. 4c and 4d show, an upper bound.

The first-order approximation is independent of L when considering the tether's efficiency and of r_C, for both payload raising and lowering from a hanging tether, and therefore differs qualitatively to the full analytical solution. When L is less than 50 km, Eqs. (11) and (12), according to Figs. 3a and 4a, agree qualitatively and quantitatively with the full solution but because of their linearity are not able to capture the curve exhibited by Eqs. (7) and (8) when L is greater than 50 km. The second-order approximation is qualitatively similar to the performance index of the full analytical solution. The quantitative discrepancy between the second-order approximation and the full solution, seen in Figs. 3b, 3d, 4b, and 4d, is small because of the choice of L and increases when L is larger. When L is less than 150 km, Eqs. (15) and (16) are in good agreement with the Δr_π of Eqs. (7) and (8). Similarly, when L is less than 50 km Eqs. (15) and (16) are in good agreement with the $\Delta r_\pi / L$ of Eqs. (7) and (8). However, as L moves above these thresholds the discrepancy between the solutions grows with increasing L. The results presented

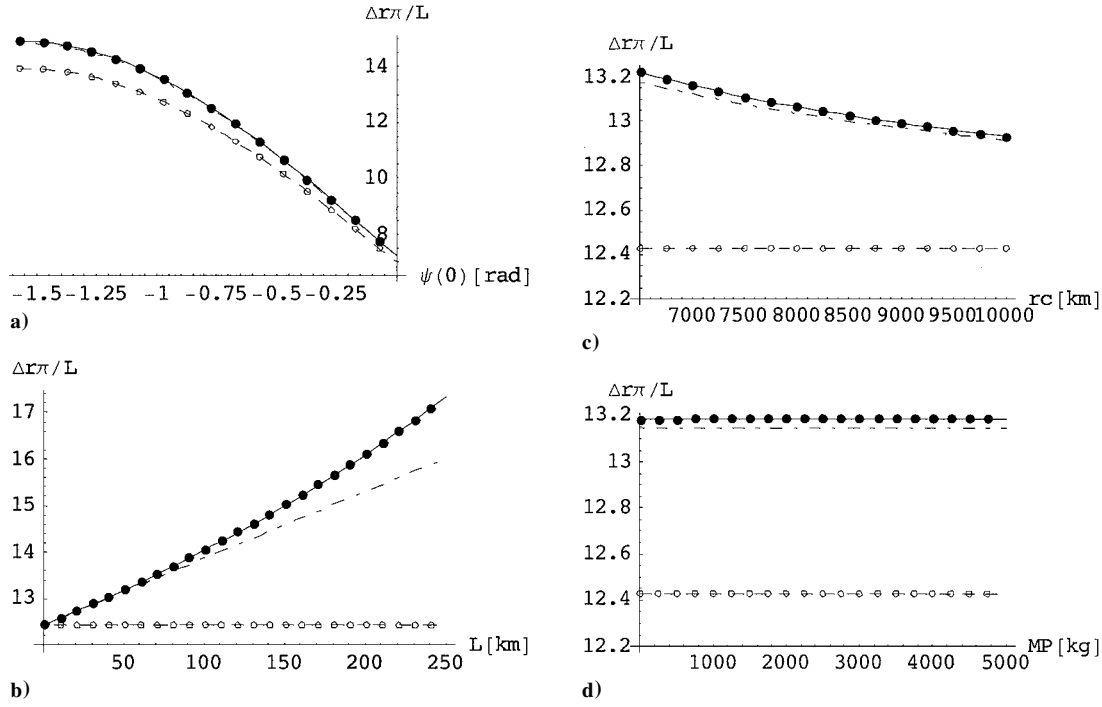

Fig. 5 Efficiency of upper payload released from a prograde librating tether: ——, analytical, Eq. (9); - - -, first-order approximation, Eq. (13); -·-, second-order approximation, Eq. (17); ●, numerical; and ○, Eq. (4).

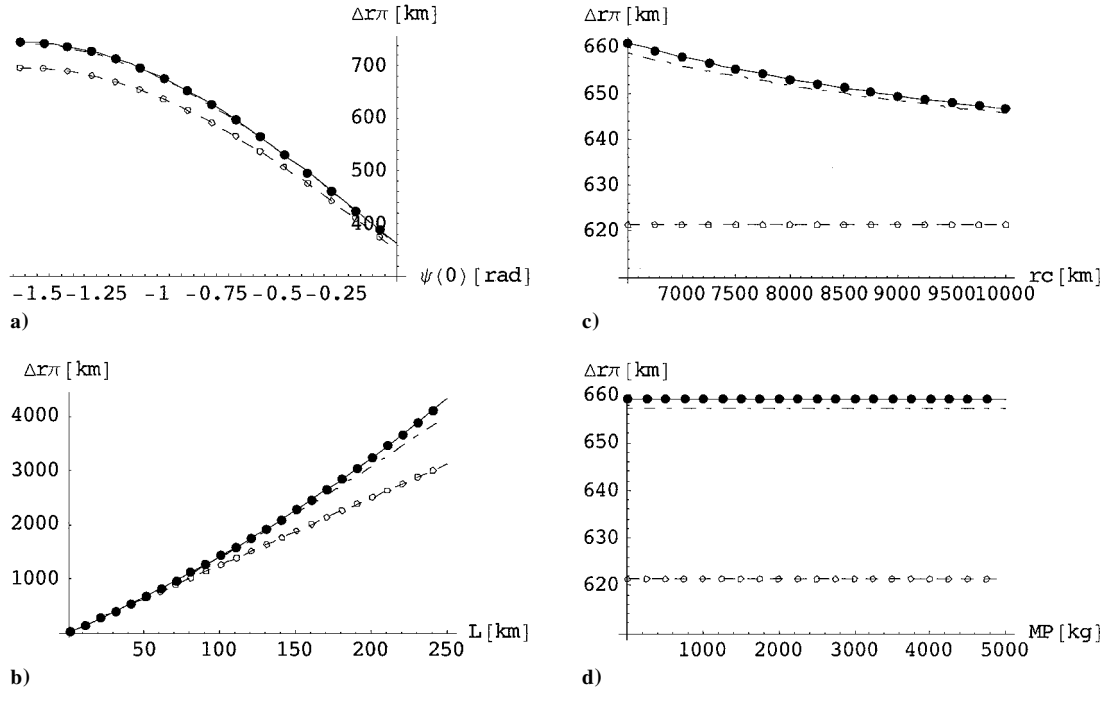

Fig. 6 Performance of upper payload released from a prograde librating tether: ——, analytical, Eq. (9); - - -, first-order approximation, Eq. (13); -·-, second-order approximation, Eq. (17); ●, numerical; and ○, Eq. (4).

in Figs. 3–12 show that the first- and second-order approximations quantitatively underpredict the tether's performance and efficiency at payload raising, whereas the first- and second-order approximations, respectively, over- and underpredict the tether's performance and efficiency at payload deorbiting. In all cases the second-order approximation is, as expected, quantitatively closer to the analytical solution than the first-order approximation and is superior to the first-order simplifications in capturing the qualitative behavior of the full nonlinear expressions.

Librating Tether

The results of the performance and efficiency of a prograde librating tether at payload raising and deorbiting are presented in Figs. 5–8, which combine the numerical simulation results, Eq. (4), and the full analytical solution, Eqs. (9) and (10), along with its first- and second-order approximations, Eqs. (13), (14) and (17), (18), respectively. These results show there is hardly any discrepancy between the full analytical and numerical results and between Eq. (4) and the first-order approximation. Despite quantitative differences, the first-order approximation is qualitatively similar to the full analytical solution when ψ_0 and M_P is varied but independent of L with regard to efficiency and r_C and thus differs qualitatively to the analytical results. When L is less than 50 km, there is good quantitative and qualitative agreement between the performance predictions of the analytical solution and its first-order approximation, but because of its linearity the approximation is unable to follow the curve

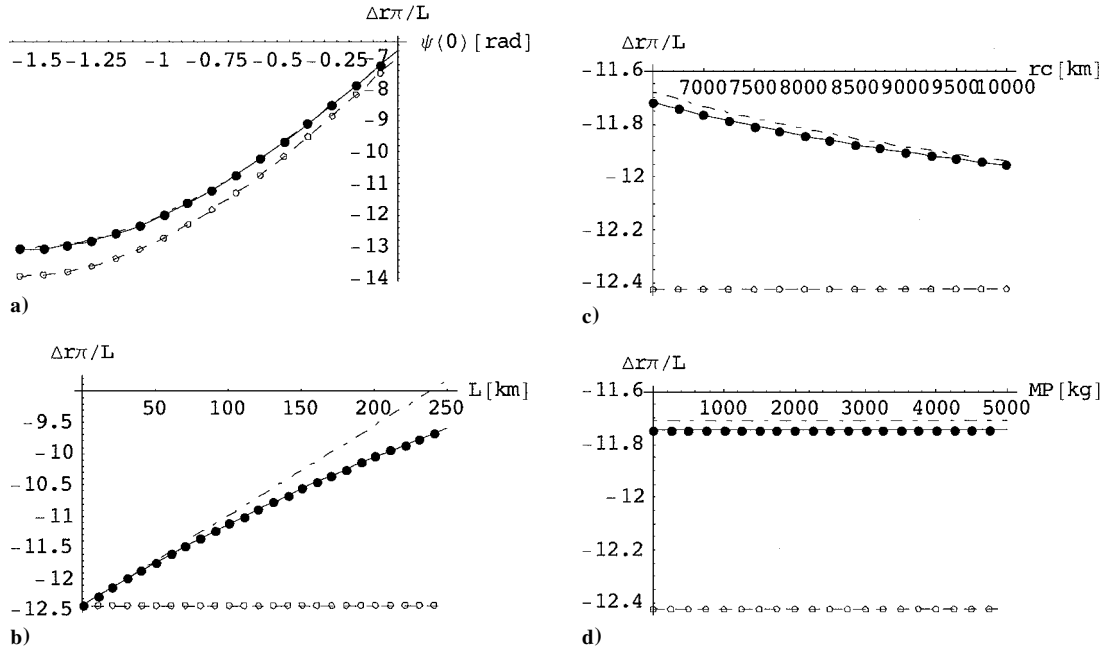

Fig. 7 Efficiency of lower payload released from a prograde librating tether: ——, analytical, Eq. (10); - - -, first-order approximation, Eq. (14); -·-, second-order approximation, Eq. (18); ●, numerical; and ○, Eq. (4).

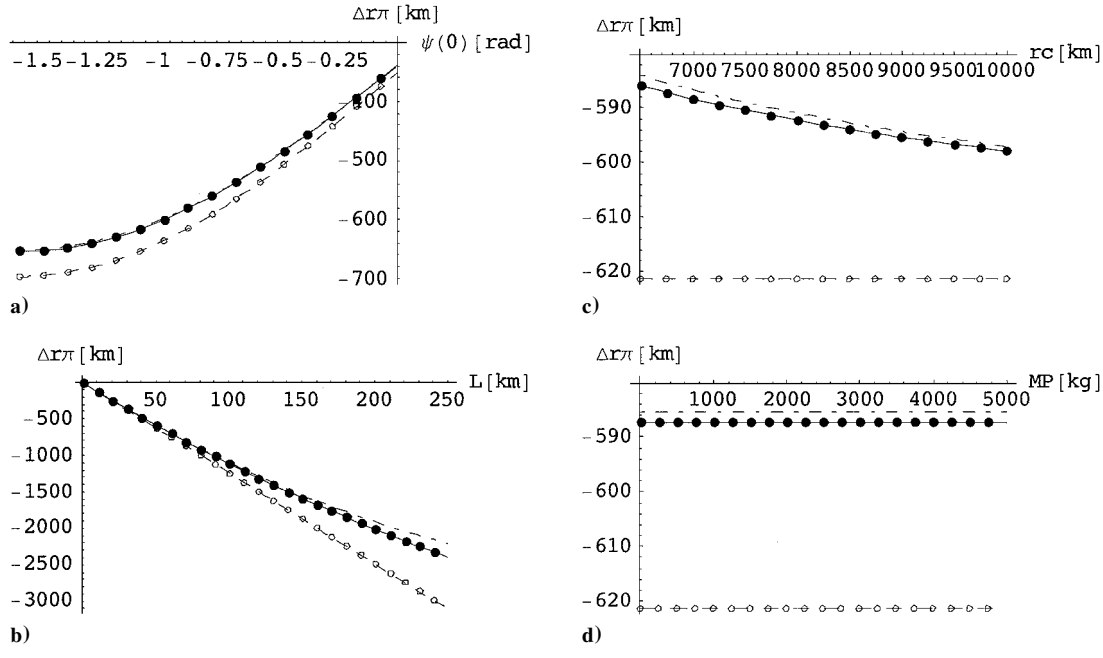

Fig. 8 Performance of lower payload released from a prograde librating tether: ——, analytical, Eq. (10); - - -, first-order approximation, Eq. (14); -·-, second-order approximation, Eq. (18); ●, numerical; and ○, Eq. (4).

of the full solution when this threshold is exceeded. The discrepancy between the analytical solution and its second-order approximation, shown in Figs. 5a, 5c, 5d, 6a, 6c, 6d, 7a, 7c, 7d, 8a, 8c, and 8d, is relatively small because of the choice of L and increases with larger L. Good agreement exists between the full solution and the second-order approximation for efficiency and performance when L is less than 50 and 150 km, respectively, but a discrepancy between these two occurs when these thresholds are exceeded and increases with larger L.

The performance and efficiency of a librating tether at payload transfer improves but also levels off with larger ψ_0; see Figs. 5a, 6a, 7a, and 8a. The results in Figs. 5b, 6b, and 8b show the performance at payload lowering and performance and efficiency at payload raising increases with larger L, but as shown in Fig. 7b larger L decreases the efficiency at payload lowering. The performance and efficiency of payload raising and lowering decreases and increases, respectively, as r_C is increased, as shown in Figs. 5c, 6c, 7c, and 8c, and is found to tail off the larger r_C becomes. The results shown in Figs. 5d, 6d, 7d, and 8d demonstrate that M_P does not significantly affect the performance nor the efficiency of the librating tether's ability at payload transfer. However, on closer inspection M_P is found to influence the numerical results, the analytical solution, and both its approximations but not Eq. (4). The performance and efficiency of payload transfer for both upper and lower payload release improves very slightly with larger M_P. For payload raising the most efficient and best performing prograde librating tether is found to be one that has the largest possible maximum libration angle and tether length as well as orbiting Earth as closely as possible. A prograde librating tether facility that has a large maximum libration angle and is situated as far as possible from Earth is very efficient and performs well at payload lowering. A long tether improves the performance, whereas a short tether improves the efficiency at payload lowering.

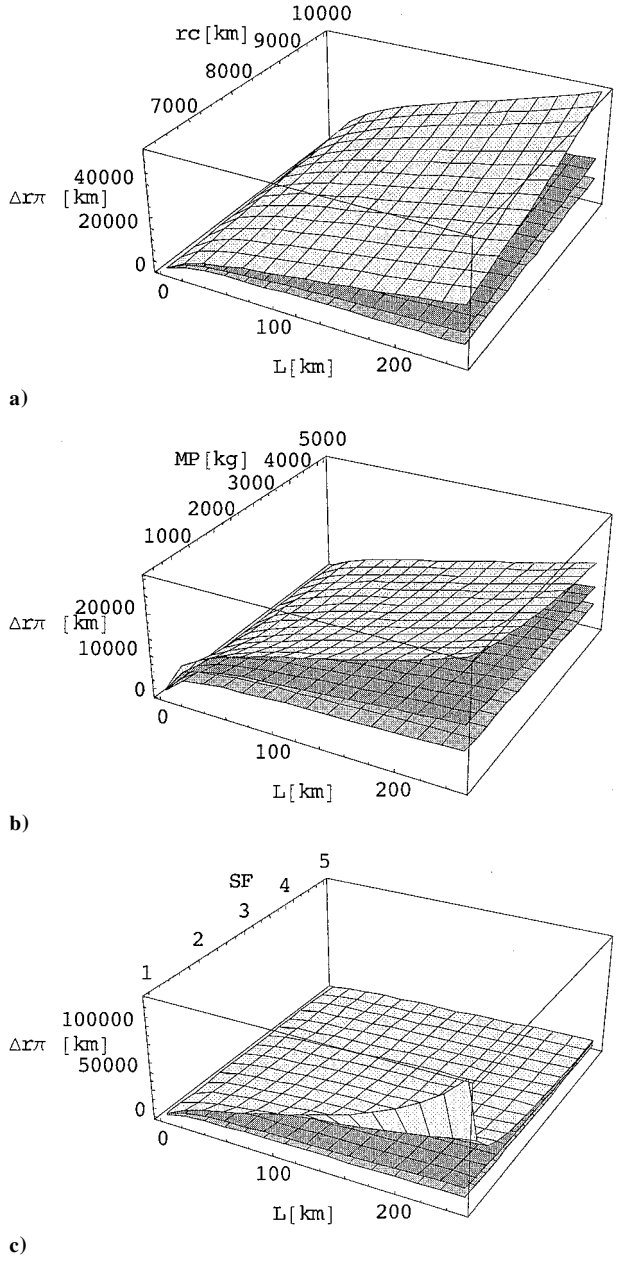

Fig. 9 Performance of upper payload released from a prograde motorized tether: light gray, analytical, Eq. (9); medium gray, first-order approximation, Eq. (13); and dark gray, second-order approximation, Eq. (17).

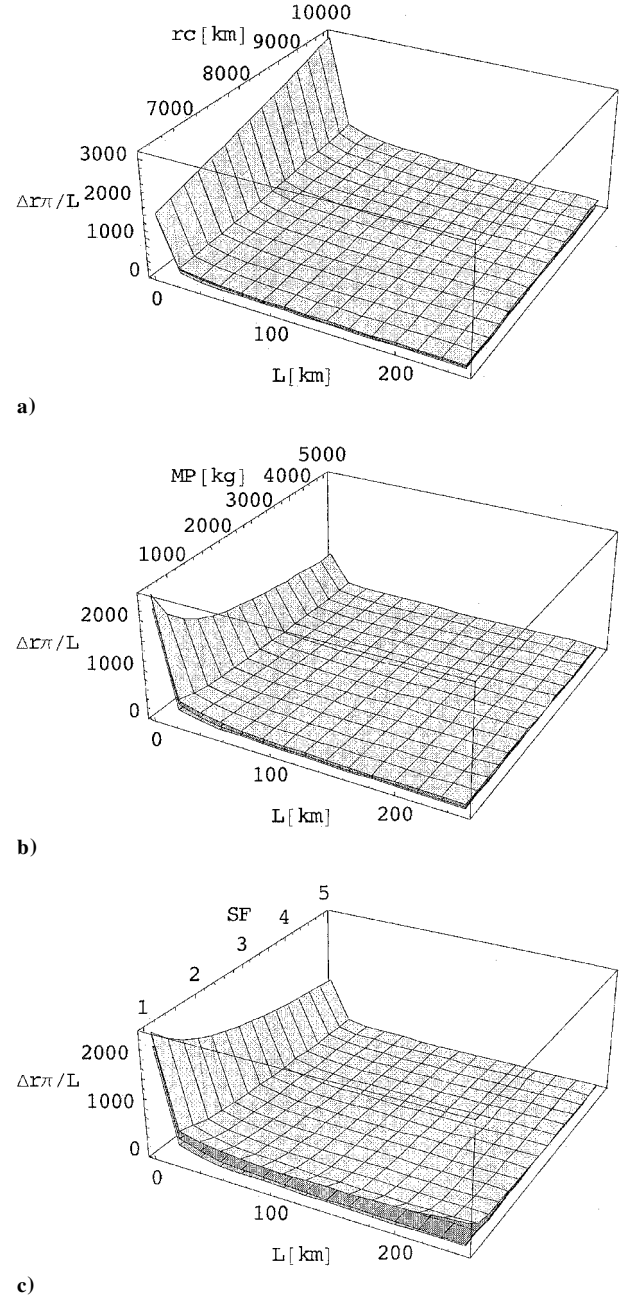

Fig. 10 Efficiency of upper payload released from a prograde motorized tether: light gray, analytical, Eq. (9); medium gray, first-order approximation, Eq. (13); and dark gray, second-order approximation, Eq. (17).

The maximum efficiency index of 14 as quoted from the literature in Eq. (2) is not found to hold according to Figs. 5a and 5b because values above 14 are readily seen to be obtained. The results show that the prograde librating tether improves, up to roughly a factor of two, on the performance and efficiency of the hanging tether.

Motorized Tether

The performance and efficiency of a prograde motorized tether at payload raising are presented in Figs. 9 and 10, which use Eqs. (9), (13), and (17). The performance and efficiency is found to improve with larger r_C and smaller S.F. and M_P. A larger L increases the performance but decreases the efficiency if the S.F. is medium or high. However, as Fig. 10c shows, when the S.F. is close to unity or if the tether's ultimate tensile stress can be increased, then the efficiency with respect to the tether's length experiences a minimum and improves with very long tethers greater than 200 km. For S.F. $= 1$ the minimum occurs for the given data at $L = 132.561$ km and is not predicted by the first- and second-order approximations. At low S.F. the approximations level off with increasing L, as seen in Figs. 9b and 9c, and fail to capture the drastically improved performance predicted by Eq. (9). Apart from these differences both orders of approximations are qualitatively similar to the full analytical solution but do underpredict the motorized tether's performance and efficiency quantitatively. The best performing motorized tether is one that can sustain very high tensile stress with a lightweight payload mass and long tether length, situated as far as possible from Earth. Unless tether lengths very much greater than 200 km are used, the most efficient motorized tether has the same configuration as for highest performance but with tether lengths that are as short as possible.

As seen in Figs. 11 and 12, which use Eqs. (10), (14), and (18), larger r_C and smaller S.F. and M_P improve the performance and efficiency of payload lowering of the prograde motorized tether. A larger L increases the performance but decreases the efficiency with no appearance of a minimum as seen with the release of the upper payload. The Δr_π achieved with motorized tethers for payload deorbiting is higher than is actually necessary in LEO where the performance of the hanging or librating tether would be sufficient. The first- and second-order approximations are both generally qualitatively similar to the full analytical solution, apart from Fig. 11c

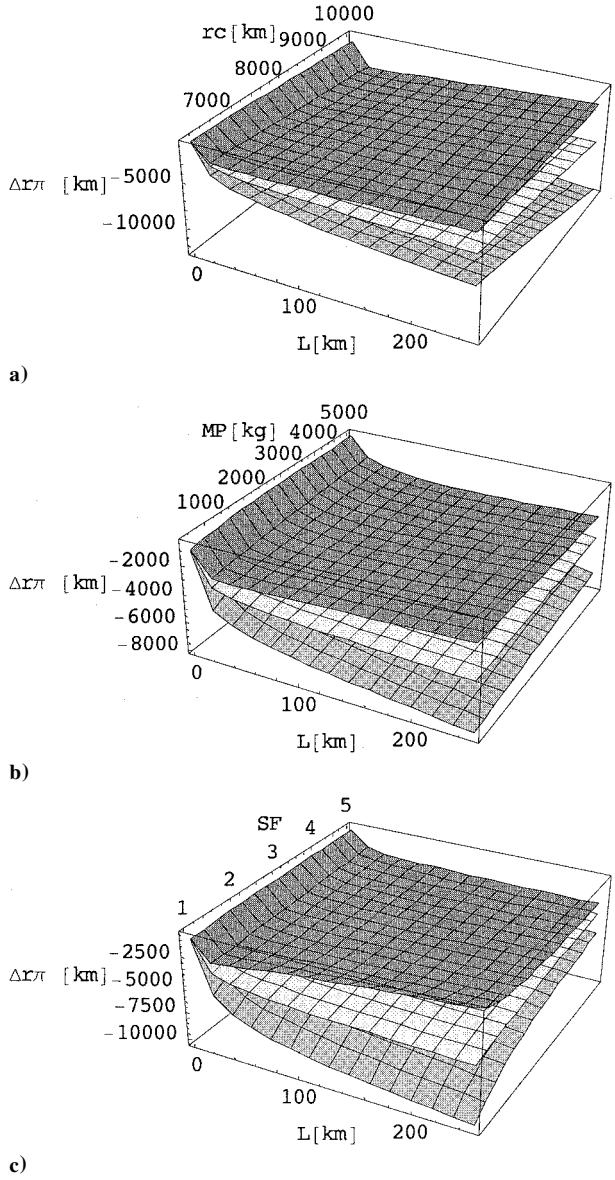

Fig. 11 Performance of lower payload released from a prograde motorized tether: light gray, analytical, Eq. (10); medium gray, first-order approximation, Eq. (14); and dark gray, second-order approximation, Eq. (18).

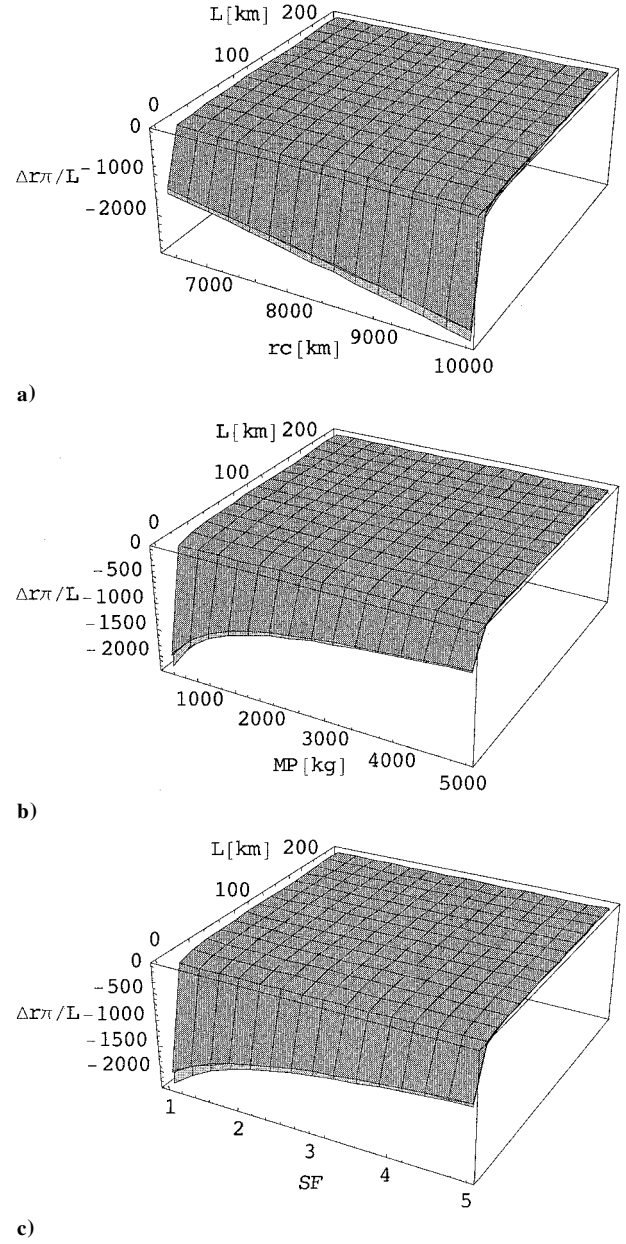

Fig. 12 Efficiency of lower payload released from a prograde motorized tether: light gray, analytical, Eq. (10); medium gray, first-order approximation, Eq. (14); and dark gray, second-order approximation, Eq. (18).

where the second-order approximation predicts the performance to improve with larger S.F. and to decrease with larger L. The best configuration for performance is to have a tether that can sustain very high tensile stresses with a low mass payload and long tether length situated as far as possible from the Earth, whereas for high efficiency the same configuration would be adopted but with short tether lengths. The motorized tether improves on the performance and efficiency of the hanging and librating tether by two orders of magnitude.

For orbital transfer the results demonstrate that either for payload raising or lowering the motorized tether performs best and is the most efficient out of the three fundamental tether motions investigated in this paper. Figure 9c shows that by using long tethers an upper payload can be propelled by a motorized tether in a circular LEO to GEO. A motorized tether using the preceding data along with $P = 5.5$ kW, $\tau = 464{,}720$ Nm, S.F. $= 1.2$, and $L = 139.122$ km can achieve $\Delta r_\pi = 35{,}467.38$ km but requires a very large motor torque and puts great demands on the tether's strength. Increasing the S.F. requires larger L and higher values of motor torque to deliver the payload to GEO. Hence, unless expendable tethers are used multiple tether stages or tethers on elliptical orbits will have to be considered. Multiple tether stages could use long tethers, which are greater than 10 km, but Figs. 10 and 12 suggest that the more efficient shorter tethers, roughly 1 km in length, are worthy of consideration. Despite the poor performance, short tethers have the advantage of being lighter, therefore, costing less to deliver into orbit, less susceptible to being severed as a result of the reduced area exposed to space debris, easier to manufacture and requiring less material, thereby, reducing costs. Generating the same tangential velocity with short tethers as achieved with long tethers requires an increase in $\dot{\psi}$ and a reduction in motor torque if the available power remains constant. Hence, the central facility's mass can be reduced as a lesser amount of torque utilizes a smaller gearbox.

The results of numerically integrating Eq. (25) to obtain the angular pitch displacement achieved from different ψ_0 over 50,000 s are shown in Fig. 13. In general, when the tether is librating then $-\pi/2 < \psi_{50{,}000} < \pi/2$ and if it is spinning progradely then $\psi_{50{,}000} > \pi/2$. The threshold between libration and spin up is obtained from Eq. (29) and shows very good agreement with the numerical results. The 50-km-long tether in Fig. 13a spins up for $-\pi/2 \le \psi_0 \le -1.3977$ rad and $1.5608 \le \psi_0 < \pi/2$ rad using $P = 5.5$ kW, whereas a 1-km-long tether driven by the same power source spins up for all ψ_0 in Fig. 13b. If $P = 55$ W, then the 1-km tether, shown in Fig. 13c, spins up for $-\pi/2 \le \psi_0 \le -1.2108$ rad

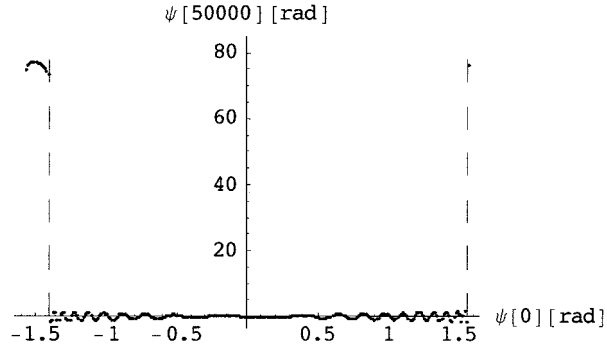

a) L = 50 km, P = 5.5 kW, τ = 193,353 Nm

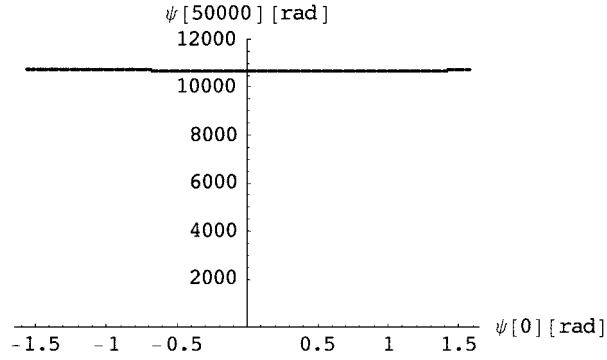

b) L = 1 km, P = 5.5 kW, τ = 17,473.1 Nm

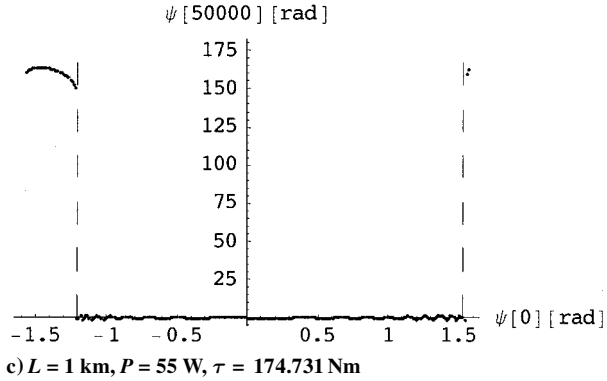

c) L = 1 km, P = 55 W, τ = 174.731 Nm

Fig. 13 Motorized tether spin-up dependency on initial angular displacement: · · · ·, numerical; and – – –, analytical criterion, Eq. (29).

and $1.5262 \leq \psi_0 < \pi/2$ rad, which is a larger region than that of the 50-km tether. Thus, a further advantage of short tethers is the ability to spin up for any ψ_0, as in Fig. 13b, and a larger region of ψ_0 for which spin up is possible if the power source is reduced, thereby, ruling out sophisticated, vulnerable, and expensive orientational controls for startup that would be required for motorized tethers using long tethers.

Rather than deploying the tethers fully before energizing the motor to spin the system, the results in Fig. 13 suggest that the motor should be energized prior to deploying the tethers. The reaction to the centripetal acceleration caused by the spinning rotor should aid deployment and increase the range of ψ_0 enabling spin up, if not altogether avoiding the problems with the resistive gravity torque at startup. Further work should model the proposed deployment and investigate the effects of tether flexibility and deployment on the performance and efficiency of the tether mediated payload orbital transfer. Furthermore, the effect of the tether releasing the payload when not aligned along the gravity vector must also be considered in future investigations.

Conclusions

Three fundamental tether motions investigated in this paper were considered for payload orbital transfer: hanging, prograde libration, and prograde motorized spin. The symmetrical double-ended motorized spinning tether performs best and is most efficient, improving by two orders of magnitude on the librating tether, which in turn improves on the hanging tether by roughly a factor of two. An upper payload using long tethers with a motorized tether on a circular orbit can be transferred from a low to a geostationary Earth orbit by employing relatively high motor torque and a safety factor on the tether strength close to unity. Multiple tethered stages or tethers on elliptic orbits will, therefore, have to be considered for geostationary payload transfer unless expendable tethers are employed. Despite their poor performance, short tethers are worth considering for use in conjunction with the multiple tethered stages because of their efficiency, overall system mass reduction, cost effectiveness, better survivability, and greater initial conditions for which spin up is possible. Consequently, the motor should be spun prior to tether deployment rather than deploying the tethers fully before commencing spin up. Finally, two common literature results, the constant efficiency index of seven for a hanging tether upper payload release and the maximum efficiency index of 14 for an upper payload released from a prograde librating tether, are found to be a lower bound and quite readily breached, respectively.

Acknowledgments

The postgraduate research scholarship awarded to S. W. Ziegler by the Faculty of Engineering, University of Glasgow, is gratefully acknowledged. The authors would like to thank D. S. Bernstein and D. I. M. Forehand for their help and advice.

References

[1]Colombo, G., Martinez-Sanchez, M., and Arnold, D., "The Use of Tethers for Payload Orbital Transfer," Smithsonian Astrophysical Observatory, NAS8-33691, Cambridge, MA, March 1982.

[2]Bekey, I., and Penzo, P. A., "Tether Propulsion," *Aerospace America*, Vol. 24, No. 7, 1986, pp. 40–43.

[3]Kelly, W. D., "Delivery and Disposal of a Space-Shuttle External Tank to Low-Earth Orbit," *Journal of the Astronautical Sciences*, Vol. 32, No. 3, 1984, pp. 343–350.

[4]Lorenzini, E. C., Cosmo, M. L., Kaiser, M., Bangham, M. E., Vonderwell, D. J., and Johnson, L., "Mission Analysis of Spinning Systems for Transfers from Low Orbits to Geostationary," *Journal of Spacecraft and Rockets*, Vol. 37, No. 2, 2000, pp. 165–172.

[5]Arnold, D. A., "The Behaviour of Long Tethers in Space," *Journal of the Astronautical Sciences*, Vol. 35, No. 1, 1987, pp. 3–18.

[6]Carroll, J. A., "Tether Applications in Space Transportation," *Acta Astronautica*, Vol. 13, No. 4, 1986, pp. 165–174.

[7]Cosmo, M. L., and Lorenzini, E. C., *Tethers in Space Handbook*, 3rd ed., Smithsonian Astrophysical Observatory, NAG8-1160, Cambridge, MA, Dec. 1997.

[8]Bekey, I., "Tethers Open New Space Options," *Astronautics and Aeronautics*, Vol. 21, No. 4, 1983, pp. 32–40.

[9]Kyroudis, G. A., and Conway, B. A., "Advantages of Tether Release of Satellites from Elliptic Orbits," *Journal of Guidance, Control, and Dynamics*, Vol. 11, No. 5, 1988, pp. 441–448.

[10]Kumar, K., Kumar, R., and Misra, A. K., "Effects of Deployment Rates and Librations on Tethered Payload Raising," *Journal of Guidance, Control, and Dynamics*, Vol. 15, No. 5, 1992, pp. 1230–1235.

[11]Cartmell, M. P., "Generating Velocity Increments by Means of a Spinning Motorized Tether," AIAA Paper 98-3739, July 1998.

[12]Cartmell, M. P., and Ziegler, S. W., "Symmetrically Laden Motorized Tethers for Continuous Two-Way Interplanetary Payload Exchange," AIAA Paper 99-2840, June 1999.

[13]Chobotov, V. A., *Orbital Mechanics*, 2nd ed., AIAA Education Series, AIAA, Reston, VA, 1996, pp. 25–27.

[14]Forward, R. L., and Hoyt, R. P., "Failsafe Multiline Hoytether Lifetimes," AIAA Paper 95-2890, July 1995.

E. Irwin
Associate Editor